

**MARbled MURRELET – WIND TURBINE COLLISION MODEL FOR
THE
RADAR RIDGE WIND RESOURCE AREA**

**Christopher S. Nations
Wallace P. Erickson**

**Western EcoSystems Technology, Inc.
2003 Central Avenue
Cheyenne, WY 82001**

Prepared for:

Energy Northwest
P.O. Box 968, M/D 1035
Richland, WA 99352

4 September 2009

EXECUTIVE SUMMARY

A simulation model (Model) was developed to assess the probability of marbled murrelet (murrelet) collision with wind turbines in the proposed development of the Radar Ridge Wind Resource Area (RRWRA). Estimated probabilities were then combined with murrelet passage rate estimates from a Hamer Environmental Inc. radar study at the RRWRA to predict the rate of murrelet fatalities under several alternative scenarios.

The Model was designed to explicitly account for murrelet characteristics, wind conditions, wind turbine design, and wind park layout. Murrelet characteristics were based on literature reviews and the results of avian data collection undertaken for the Project. These characteristics included physical dimensions and flight altitude, speed, and direction. A key aspect of modeled murrelet behavior was avoidance probability, with separate values used for active rotors and stationary structures. Three alternative wind turbine designs were examined, based on best available technical information. Modeled wind turbine features included dimensions of towers (height was 80 m for all designs), nacelles, and blades (in 3-D), as well as operational properties. In cases where precise operational properties were not available or were non-conservative, assumptions were modified as appropriate. Wind park layouts followed turbine design, either a larger string of small wind turbines or a shorter string of medium or large turbines. Other Model conditions included season, time of day, and a curtailment (temporary shut-down) strategy. In simulations, the outcome of each murrelet flight was either successful passage through the wind park or fatal collision. The proportion of all flights that resulted in collision represented an estimate of collision probability.

Results showed that mean collision probabilities ranged from 0.00016 to 0.00056, such that 16 to 56 of every 100,000 murrelet flights would be expected to result in collision. Mean collision probabilities were similar for the small and medium wind turbine designs, and somewhat greater for large turbines. Morning and evening flight periods during the breeding season showed little difference in collision probability, while risk of collision was substantially higher in winter than in the breeding season, due to higher winter wind speeds and, thus, higher rotor speeds. Furthermore, curtailment substantially reduced collision probability.

Passage rate estimates from the radar study at the RRWRA were adjusted upwards to account for flock size (each murrelet-type target represents more than 1 individual, on average) and incomplete radar coverage of the ridge-top Project area. Predicted fatalities generally reflected the patterns in collision probabilities, though there was one notable exception. Despite higher collision risk in winter, passage rate was lower in winter than in the breeding season, so that there was very little seasonal difference in predicted fatality. In the worst case examined for large wind turbines (conditions including no curtailment), predicted annual fatalities were 0.72, or approximately 1 fatality every 1.4 years. Curtailment during the breeding season flight periods led to fewer than 0.6 fatalities per year with the large turbines. For small turbines, there were 0.55 predicted fatalities per year under no curtailment and fewer than 0.5 fatalities per year under curtailment during breeding season flight periods.

The simulations provide information concerning the likelihood of murrelet take. These simulations make use of the best available scientific and commercial information regarding murrelet behaviors and abundance near the Project area, as well as other studies of avoidance by other similar species. In view of the very small estimates derived from the modeling work over the life of the Project, even under very conservative assumptions, the amount of take is expected to be very low.

In our initial report on the simulation model (October 2008), we included estimates of fatality rates that were lower than the current estimates. We have made many changes to the model since that time to account for the best available data, as well as a range of possible operating conditions (e.g., wind turbine design and wind park layout) as recommended in the Incidental Take Permit Application. As examples, these changes include: representation of wind turbine blades as 3-dimensional rather than 1-dimensional structures; a separate sub-model for collision with stationary rotors whereas previously we assumed zero collision probability; the addition of a third turbine design with a larger rotor; the elimination of wind park avoidance (flight diversions to the side or above the entire wind park); a revised function relating turbine speed and wind speed based on operational data rather than manufacturer specifications; and, an adjustment for flock size (under the assumption that murrelet-type targets represent more than 1 murrelet). Most of these changes have contributed to larger estimates of either collision probability or passage rate and, thus, to larger fatality estimates. At the same time, we have retained values for avoidance probabilities of active rotors and stationary structures that we believe are conservative, as the assumption of lower avoidance contributes to higher predicted fatality. However, even with the numerous model changes, predicted fatalities may be under 0.5 per year. These estimates are based on the best available science and a set of conservative assumptions.

Cooper (2008) reviewed a preliminary version of this report (West Inc., 2008). Excepting those few cases where Cooper (2008) had no suggestions (e.g., accounting for murrelet attraction to turbine lighting), the current version of the model incorporates changes prompted by his review. Additional comments from the Technical Advisory Committee (including USFWS, WDNR, and WDFW) have also been incorporated as changes in the simulation model.

INTRODUCTION

An individual-based mathematical model has been developed for the estimation of the probability of marbled murrelet (*Brachyramphus marmoratus*) (hereafter, simply “murrelet”) collisions with wind turbines in the Radar Ridge Wind Resource Area (RRWRA). The model incorporates Tucker’s (1996) approach for estimating the probability of a bird colliding with the rotor blades of a wind turbine. In addition to collisions with active rotors, the model allows for estimating the probabilities of murrelets colliding with stationary rotors and with the wind turbine tower and nacelle. The physical and dynamic characteristics of the proposed wind turbines as well as the spatial arrangement of the individual wind turbines within the wind park are incorporated in the model. Murrelet characteristics including size, flight altitude and speed, and avoidance behaviors are incorporated based on literature reviews and the results of the avian data collection undertaken for the project. Wind characteristics are based on data collected from a meteorological tower at the site. Collision probabilities are assessed by simulating flight paths of individual murrelets through the wind park and calculating the proportion of all such paths that resulted in collision. Temporal variability in both wind conditions and murrelet flight patterns are accounted for by explicit modeling of season and time of day.

Predicted numbers of fatalities are then calculated by multiplying collision probabilities by passage rates estimated from marine radar surveys. As described in Hamer’s (2009) RRWRA radar study, it is not possible to ascertain with certainty whether all radar targets are truly murrelets or whether some targets may be other avian species with similar flight characteristics. Therefore, summaries of passage rate, flight altitude, and flight direction based on radar data refer to “murrelet-type targets”. We are confident that the inclusion of non-murrelet targets leads to over-estimates of murrelet passage rates that are consequently reflected in fatality predictions. While the simulation model necessarily uses mathematical constructs to represent birds, its intent is to address collision probability for a real species. Therefore, where the model is concerned, we refer to “murrelets”.

Results presented here represent an analysis based on a number of simplifying assumptions described in greater detail below.

ASSUMPTIONS AND MODEL SET-UP

Seasons and Periods of the Day

Seasons and periods of the day were determined based on a literature review of murrelet biology (Hamer Environmental). In some cases, dates were adjusted to account for latitudinal differences between the published study sites and RRWRA. Furthermore, modeling made it necessary to set clear boundaries between seasons, and similarly, between periods of the day, although murrelet activity may vary. The breeding season was defined as April 20 – August 14, while winter was defined as October 16 – April 19. Adults were assumed to be flying during these 2 seasons only. During molt (August 15 – October 15), flight does not occur, and therefore this season was not explicitly included in the model.

During most of the year, flights were assumed to occur only in the morning during a 3-hour period around sunrise. This period was defined as 04:00 – 07:00 for the breeding season, and 05:00 – 08:00 for winter. Additional evening flights were assumed to occur during the peak of the breeding season, defined to be the month of July only, for the 3-hour period 20:00 – 23:00.

These seasons and periods of the day were used both for sampling wind conditions in the simulation model (see *Wind Characteristics* below), and for determining passage rates from radar observations (see *Passage Rate Estimation* below).

Wind Turbines

We considered 3 alternative wind turbine designs and associated wind park layouts (see *Wind Park* below). The larger 2 wind turbines were both Vestas V90 rated at 3.0 MW, one with a 101.5 m diameter rotor and the other with a 90 m rotor. The smallest of the 3 designs was the General Electric 1.5sle rated at 1.5 MW, with a 77 m rotor. Characteristics of these wind turbines (Table 1) were based on company specifications to the extent possible (some specifications are proprietary), supplemented in some cases by third party specifications re-scaled to the appropriate dimensions. In addition, some simplifications were introduced to facilitate modeling. These wind turbines were chosen as representative of various possible designs, though the wind turbines that are ultimately used may be different. Hereafter, these alternatives will be referred to as simply the large, medium, and small wind turbines.

Each tower was modeled as a monopole with diameter that tapered smoothly (rather than in stepped fashion) from the base to the top. The tower cross-section was represented as an octagon, rather than a true circle. Two separate sub-models were used for rotors depending on wind conditions and wind turbine dynamic characteristics (described below). The Tucker (1996) model (see detailed explanation in later section; *Tucker Model for Turning Rotors*) was used to calculate probability of collision with the rotor structure when wind conditions were such that rotors would be turning. For stationary rotors, a 3-dimensional geometric model was used to determine collision probability under conditions of no wind, very high wind speeds, and curtailment (a mitigation strategy designed to minimize murrelet fatalities during periods when passage rates are particularly high). Additional details of rotor structure assumed for each sub-model are described below (see *Flight Through Rotors*).

The dynamic relationship between wind speed and wind turbine rotational speed was based on data from operating wind turbines (another manufacturer, but similar design features) at another wind project. To account for the differences in rated wind speeds and rated rotational speeds, these data were re-scaled to match the characteristics of the 1.5 MW and, separately, the 3.0 MW wind turbines. A cubic spline was fit to each of the re-scaled datasets (Figure 1). In brief, operational data indicate a rapid increase in rotational speed with increase in wind speed, except for a shoulder in the region of the cut-in speed. Note that the plateau at the rated rotational speed is reached at wind speeds somewhat lower than the nominal rated wind speed. More generally, the use of the spline function fit to operational data results in a more conservative relationship than would be obtained from strict interpretation of manufacturer specifications. That is, operational data generally indicate higher rotational speed (and, thus, higher risk of collision) at given wind speed than is indicated by specifications. Otherwise, at very high wind speeds where

operational data were limited, the fitted spline functions were augmented with a sharp decrease from rated rotational velocity to 0 RPM in the region where wind exceeded the cut-out speed (the rotor is disengaged for safety reasons at high wind speeds). The blade pitch angle was assumed to be constant at nearly 0° up to 12.7 m/s (approximately 2 m/s below the rated wind speed), and then increase rapidly up to the cut-out speed (Figure 1) following a pattern described by Hansen et al. (2005) and confirmed by operational data. When the rotors were not turning (above cut-out speeds), the blades were pitched out of the wind at 90° (not shown in Figure 1).

Curtailment

A wind power curtailment strategy was simulated to examine the effects on murrelet collision probabilities and predicted fatalities. This strategy would entail cessation of power generation by feathering the rotor blades to disengage the wind turbines. The presumption is that collision risk would be lower for murrelets. Curtailment was only considered for the breeding season (April 20 – August 14) when passage rates are greatest, and then only during the flying periods of the day – either the morning period (04:00 – 07:00) alone, or both the morning and evening (20:00 – 23:00) periods. For each of these options, shut-down would occur following an “80/80” strategy. These numbers indicate that on 80% of days and, on those days, during 80% of the period (either morning, or both morning and evening) shut-down would occur. Thus, under the morning-only 80/80 strategy, 64% of breeding season morning flights through the wind park would occur during periods when wind power generation was curtailed. Curtailment was simulated by treating the rotors as stationary – irrespective of wind conditions – for 64% of flights during the appropriate period(s) of the day.

Wind Park

The proposed layout of the RRWRA consists of a single string of regularly spaced wind turbines oriented approximately along a Northwest-to-Southeast line (Figure 2). With the 3 MW design (both the large and medium sizes) there would be 27 wind turbines, while the layout for the small 1.5 MW design would entail 32 wind turbines. In both cases, the configuration of wind turbines has been determined to optimize energy extraction and satisfy other constraints (primarily buffer zones around communications towers and property boundaries). Some changes to the layout may occur before final design, but these changes are not anticipated to lead to appreciably different model results.

Wind Characteristics

Observed Wind Data

Wind data were available from 4 meteorological towers in the RRWRA. Tower 801 was equipped with instrumentation at 27 m height that was operating nearly continuously from early April 2005 through late May 2009 (with a prolonged gap in operation from mid-November 2007 through mid-April 2008). Towers 802, 803, and 804 had instrumentation at 20 m, 35 m, and 50 m that provided data for the period from January through June 2008. Tower 801 was treated as the primary source of data because of its year-round operation for a total of nearly 4 years.

Data from Towers 802 – 804 were used to estimate the power law relationship (Elliot et al. 1986) that describes increase in wind speed occurring with increase in height above the ground. Least squares optimization was used to estimate the exponent, α , in the equation $V_2 = V_1(h_2/h_1)^\alpha$ where V_1 and V_2 were measured wind velocities and h_1 and h_2 were measurement heights at lower and higher elevations, respectively. In general, the exponent depends on several factors including ground surface roughness and solar insolation. The exponent for these 3 towers was estimated using the 35 m and 50 m wind measurements (values at 20 m may have been influenced by surrounding trees). The average of these 3 estimates was $\hat{\alpha} = 0.21$. Finally, wind speed measured at 27 m (V_1) on Tower 801 was adjusted to obtain approximate wind speed at 80 m (V_2), using $V_2 = V_1(80/27)^{0.21}$ or $V_2 = 1.256V_1$. Eighty meters represents the presumptive hub height (Table 1) and is likely more representative of the wind velocities encountered by both wind turbine rotors and murrelets at risk of collision.

Measurements of wind speed and direction were obtained at either 10-minute or 1-hour intervals. The 10-minute values were averaged to obtain a single value for each hour. Directional averages were estimated using $\bar{\mu} = \tan^{-1}(\bar{y}/\bar{x})$, where $\bar{y} = \sum_{i=1}^6 \cos(\theta_i)/6$, $\bar{x} = \sum_{i=1}^6 \sin(\theta_i)/6$, and θ_i was the direction for the i^{th} observation (Batschelet 1981). Wind speed and direction showed both diurnal and seasonal variation (Figures 3-5). In general, wind speed was lower and less variable in the breeding season than in winter (Figures 3 and 4). Furthermore, wind speed was somewhat higher in the evening during July (peak breeding season) than in the morning over the entire breeding season (Figures 3 and 4). Wind direction was typically from the West and Southwest in the morning during the breeding season and from the Northwest in the evening during July, while in the winter winds were generally from the East and Southeast (Figure 5).

During simulations (described in greater detail below), hourly wind observations of direction and height-adjusted speed were randomly sampled from the available data for a particular season and period of the day.

Murrelet Characteristics

Size and Speed

Murrelets were assumed to have wing span of 0.41 m and body length of 0.25 m (Sibley 2003). Body size was held constant for all individuals in all simulations.

Simulated flight speeds were based on a radar study in British Columbia that entailed measurement of speed of 3000 independent murrelet flights (Elliot et al. 2004). The simulation distribution was designed to mimic the observed frequency histogram (Figure 1b in Elliot et al. 2004) and the associated sample mean of 22.6 m/s. The observed distribution was approximated by adding the value 10 to random variates from a Gamma(4.8, 2.6) distribution (Figure 6).

Murrelet flight was simulated to maintain constant air speed given by the randomly selected speed. Ground directions were based on radar data as described below (see *Flight Direction*). Ground speed and flight direction with respect to the wind were determined using the vector relationship $\mathbf{v}_g = \mathbf{v}_w + \mathbf{v}_a$ where \mathbf{v} represented velocity (both direction and magnitude), g represented murrelet flight with respect to the ground, w represented wind, and a represented

murrelet flight with respect to the air. If the murrelet's selected air speed led to ground speed less than 1 m/s, then the air speed was increased so that the resultant ground speed was exactly 1 m/s. If the newly calculated air speed exceeded the defined maximum speed (51 m/s), then flight ceased. Necessarily, there were no collisions for that iteration.

Flight Direction

Recent site-specific radar studies (Hamer Environmental 2009) determined flight directions (with respect to the ground) of murrelet-type targets within the RRWRA. Directions were measured for 71 murrelet-type targets in summer (2007, 2008, and 2009) and 17 murrelet-type targets in winter (2008 and 2009). Rose plots (Figure 7) indicate that flight directions were widely distributed in summer, though a high proportion of targets flew from the East. In winter, no targets were flying from the North, though otherwise directions appeared widely distributed. Note that data shown in Figure 7 have been filtered. Radar targets headed North (between 337.5° and 22.5°) during March – May were considered to be migrating waterfowl, while targets headed Southeast-to-South (between 135° and 180°) in July were considered to be shorebirds transiting inland. All such targets were removed from the analysis dataset.

Because sample sizes were small, particularly in the winter, and because observed distributions were not unimodal, it was difficult to fit parametric distributions to the observed directions. Therefore, continuous distributions were constructed (Figure 8) based on qualitative assessments of the observations (Figure 7). Breeding season flight directions were represented by a mixture of 3 von Mises distributions with the strongest mode from the East and the weakest mode from the Southwest. Winter flight directions were represented by a cardioid distribution, similar to a uniform distribution, but having greater probabilities for flights from the South.

During simulations, each murrelet flight was randomly assigned a direction with respect to the ground as appropriate for the selected season. Assigned direction was fixed during each simulated flight. That is, flight path direction did not change in response to wind or other conditions. Encounter with wind turbine structures could induce temporary changes in direction if the structure was avoided, but original direction was maintained following avoidance. Flight directions with respect to the wind were calculated using the vector relationship $\mathbf{v}_g = \mathbf{v}_w + \mathbf{v}_a$ as described above. These flight directions were critical in estimating rotor collision probabilities under the Tucker (1996) model.

Flight Altitude

Using radar, Hamer Environmental (2009) estimated minimum flight altitudes for 37 individual murrelet-type targets flying within the RRWRA (Figure 9). A Lognormal(5.57,0.558) distribution was fit to these data, with particular emphasis on fitting altitudes below projected maximum rotor height (Figure 9). A comparison of the observed and lognormal distributions (Table 2) shows that they have similar means and standard deviations, and both have similar percentiles in the left tails, the region of the distributions within wind turbine heights. During model simulations, flight heights were generated as random variates from the specified Lognormal distribution.

Avoidance

Murrelet avoidance may occur at several levels. Recent studies of offshore wind projects in Denmark (Peterson et al. 2006) provide strong evidence that an entire wind park will be avoided by some species. In a simulation such avoidance could reasonably be envisioned as flight changes that either resulted in murrelets traversing above the wind park, or around one side. While our model is capable of incorporating this level of avoidance, we chose not to include it, in effect, by setting wind park avoidance probability equal to 0. Thus, all simulated flights were directed at the wind park, though a large proportion were at heights above the presumed wind turbine maximum extended blade-tip height (see *Flight Altitude* above).

If a simulated flight path entered the wind park within wind turbine height, then avoidance was evaluated as individual structures – either rotor, tower, or nacelle – were encountered. While failure to avoid a tower or nacelle necessarily resulted in a collision, failure to avoid the rotor-swept area did not imply a collision. Encounter of the rotor-swept area invoked either the dynamic Tucker (1996) model or a 3-dimensional geometric model for stationary rotors. Either rotor model might allow a murrelet to pass unharmed. Furthermore, the Tucker model incorporated a safety zone allowing a murrelet to pass near the hub with lower probability of collision, however conservative refinements have been implemented (described in greater detail below). We simulated separate avoidance values for each of the primary components (rotor and tower/nacelle avoidance). This approach allowed an assessment of the relative contribution of each component to collision probability.

Tower and Nacelle Avoidance

Tower and nacelle avoidance probabilities were simulated at 0.90. In clear conditions, avoidance of fixed structures is likely to be extremely high (very close to 100%). Lower avoidance probability accounts for less ideal conditions (e.g., heavy fog and/or low light). In simulations of murrelet flight, tower avoidance was implemented by resumption of the same flight path on the opposite side of the tower (as if the murrelet detoured around the tower but otherwise maintained direction and altitude). Nacelle avoidance was implemented by increasing flight altitude sufficient to clear the structure by 1 m but otherwise maintaining the same direction. Following such avoidance, altitude was held constant until potential encounter and avoidance of another structure.

We note that these implementations of stationary structure avoidance are fairly conservative. Avoidance of a tower in the model has no effect on the murrelet's chances of encountering another structure, because altitude and heading are unchanged. Nacelle avoidance does affect the probability of encountering another nacelle or tower; because of the altitude change, the subsequent chance of encounter is zero. However, the overall chances of encountering another structure are changed very little because (1) towers and nacelles are not likely to be encountered in any case due to their relatively small frontal area, and (2) the murrelet's resultant altitude remains well within rotor heights and rotors occupy a much larger area.

Rotor Avoidance

In simulations of murrelet flight, rotor avoidance generally was implemented by altering flight altitudes, but otherwise maintaining the same course. Altitude was adjusted directly up or down, depending on which edge of the rotor disc was nearest to the point of intersection (Figure 10). The adjustment was sufficient to clear the disc edge by 1 m. An upward adjustment would not necessarily yield an altitude greater than maximum rotor height. In fact, this would likely not occur unless the flight path was directly above (or nearly so) the hub. Thus, successful avoidance of a rotor would not necessarily eliminate risk of collision with another wind turbine. Furthermore, after successful avoidance, flight altitude was not altered until another structure was encountered and then possibly avoided.

The only exception to the general flight pattern described above occurred when a flight path was parallel to the plane of the rotor (i.e., perpendicular to the wind if the wind was blowing). For the infrequent cases in which the flight path intersected the edge of the rotor disc, avoidance was implemented as for towers (as if the bird detoured around the rotor but otherwise maintained direction and altitude). Again, this implementation is conservative in that avoidance has no effect on a bird's chances of subsequently encountering another structure.

The avoidance probability for active rotors (turning rotors under suitable wind conditions and no curtailment) was simulated as 0.75. For stationary rotors (not turning either due to unsuitable wind or curtailment), avoidance probability was 0.9, the same as for towers and nacelles.

Flight Through Rotors

Failure to avoid the rotor necessarily meant that a murrelet passed through the rotor disc. Of course, such a flight path would not necessarily result in a collision. As briefly described above, two separate rotor models were employed, depending on wind conditions and corresponding wind turbine dynamic characteristics, and also on curtailment strategy. By design, if wind speed is above the wind turbine cut-out speed, then the rotor ceases to turn. (In principle, the same response occurs below the cut-in speed, though in real-world conditions, on average, wind turbines maintain low rotational velocities even at low wind speeds, as shown in Figure 1.) Otherwise, in simulations of curtailment, rotors were held stationary a certain percentage of the time, even when wind conditions were sufficient for power generation. To estimate collision probabilities in those situations, we constructed a 3-dimensional geometric model of the rotor alone (hub and blades). With an active rotor (wind speed below the cut-out speed), estimation of collision probability with the rotating blades was somewhat more difficult. For that situation, we relied on the Tucker (1996) model.

Geometric Model for Stationary Rotors

Estimation of collision probability with a stationary rotor relied on a 3-dimensional geometric model. The model was based on a small set of blade measurements that were provided by wind turbine manufacturers supplemented with several measurements that we assumed (Table 1). No blade twist was used, blade pitch was fixed at 90° to the plane of the rotor disc, and chord length was set to decrease linearly between the maximum chord and the tip chord (Table 1). Additional

simplifying geometric assumptions led to a rotor model comprised of 39 polygons (Figure 11). Preliminary simulations were conducted in which birds were represented as 1-dimensional points (as in the main model). Thousands of birds were directed at the rotor from all angles of approach. The proportion of birds that intercepted any polygon of the rotor was taken as an estimate of collision probability. Average collision probability was calculated as a function of both approach angle (the angle between a flight path and the plane of the rotor) and radius (distance of the intersection point from the center of the rotor). Results were summarized in a lookup table of collision probabilities where columns represented approach angle (in 1° increments) and rows represented radius (in increments of approximately 0.4 m). In simulations, whenever a murrelet-type target's flight path intersected a stationary rotor, both the relative angle of approach and the radius were assessed. These 2 values were used to enter the lookup table and retrieve a probability of collision.

Tucker Model for Turning Rotors

As expressed by Tucker's (1996) model, the probability that a bird will collide with the leading edge of a rotor blade depends on the following factors: (1) bird air speed; (2) bird size; (3) angle of approach (relative to the wind); (4) wind speed; (5) blade angular speed; (6) location on the rotor disc that is intersected by the flight path; and, (7) the axial induction factor (*AIF*). These parameters are sufficient to calculate collision probability in what Tucker called the 1-dimensional model (because the blades were considered to be 1-dimensional, i.e., straight lines representing the leading edges). In a further refinement, Tucker considered blades with both width, characterized by chord length, and variable twist such that they occupied 3-dimensional space. This was termed the 3-dimensional model, though no thickness was attributed to the blades. Given chord length and twist angle for a particular radius along the blade, the additional model components allow calculation of probability of collision with the trailing surface of the blade. The total collision probability was calculated as the sum of the separate components: a bird might collide with either the leading edge or the trailing surface.

Figure 12 depicts example probabilities of collision with the rotor blades of the medium wind turbine (3.0 MW, 90 m rotor) in both downwind and crosswind flights. For this figure, murrelet selected airspeed was set at 22.6 m/s (the mean observed by Elliot et al. 2004) and wind speed was set at 8 m/s, which was the mean speed (adjusted to 80 m height) throughout the entire year as measured at Tower 801 on the ridge-top. Note that predicted collision probabilities have near circular symmetry in downwind flight, though there is slight asymmetry: at a given radius, collision probability is somewhat higher directly above or below the hub than directly to either side of the hub. Generally for downwind flight, collision probability is very low at the periphery of the rotor and increases toward the hub. For upwind flight (not shown in Figure 12), the shape of the contours is very similar to those for downwind flight, though probability of collision at any point on the disc is higher in upwind flight because residence time within the disc is greater.

Probability contours are more complex for crosswind flight (Figure 12). In the example shown, the bird's air velocity is perpendicular to the wind velocity, from the left, and the resultant ground velocity carries the bird through the rotor at an oblique angle. If the bird enters the rotor disc above the hub, collision probability is relatively low because the bird's flight and the clockwise rotation of the rotor tend to be in the same direction (Tucker referred to the blades in

this situation as “following”). On the other hand, below the hub collision probability is high because the bird flight and rotor direction tend to be opposing (“approaching” blades). Irrespective of flight direction, the pattern of collision probabilities within the rotor disc is largely determined by the relative geometry of the blades and the bird, which is assumed to maintain constant orientation (i.e., wings parallel to the ground; body does not roll, pitch, or yaw).

For modern variable speed wind turbines, the factors of wind speed and blade angular speed are interacting effects since wind speed affects both rotor speed and a bird’s residence time in the plane of the rotor. *AIF* represents the loss of wind energy (and velocity) due to capture of energy by the wind turbine. Tucker assumed $AIF = 0.25$ and noted that if a wind turbine were operating at maximum efficiency, then $AIF = 1/3$. This property is not known for either of the wind turbine designs proposed for the RRWRA. Therefore, *AIF* was held constant at 0.25 as in Tucker (1996). *AIF* is certainly related to rotor collision probability, with higher values (up to a maximum of 0.33) leading to higher collision probabilities because of greater wind energy loss to the wind turbine, and thus, longer bird residence times within the plane of the rotor. Conversely, lower *AIF* would lead to lower probabilities of collision. In the absence of better information, $AIF = 0.25$ seems to be a reasonable choice. Previous analyses using this collision model have indicated that sensitivity of collision probability to *AIF* (particularly in the range between 0.25 and 0.33) is extremely low (negligible in comparison to avoidance probabilities, for instance).

For the 3-dimensional component of the model, blade chord lengths were assumed to decrease linearly with radius from the maximum chord to the tip chord. Blade twist angles were based on data for the smaller Nordtank 500/41 (Hansen 2008) using re-scaled blade radii (Figure 13). Unlike the relationship shown in Figure 13, twist angle is undefined between the hub and the maximum chord. However, with no twist, there is no additional component to account for collision behind the leading edge of the blade near the hub (recognizing that “edge” does not accurately describe the rounded shank). An ad hoc adjustment was made to compensate for this model feature and thereby allow finite probability of collision on the trailing surface. In particular, the maximum twist angle was assigned to the blade near the hub, including the portion representing the shank. We believe this is a conservative adjustment, likely to somewhat overestimate collision probability near the hub. Certainly, it yields higher collision probabilities than the unmodified Tucker model.

Blade avoidance

Both *selected* and *maximum* air speeds of birds play a role in determining collision probability. The selected speed for each murrelet flight is chosen by generating a random variate (as described above in the *Murrelet Characteristics / Size and Speed* section), while the maximum speed is fixed for all murrelets. The selected speed determines the amount of time that the bird is within the plane of the rotor. Maximum speed is related to what Tucker referred to as “tangential threshold speed of the blade”, but as he made clear, this speed is a property of both the bird and the wind turbine. Tangential threshold speed is “meant to represent the behavior of real birds, which are able to avoid collisions by flying around slow-moving objects, such as the blades near the rotor hub.” By temporarily increasing speed (to the maximum value), birds can avoid

collision near the hub. Higher maximum speeds increase the size of the safety zone around the hub. In our model, this behavior is termed “blade avoidance”.

Tucker (1996) assumed zero probability of collision within the safety zone if blade avoidance was enabled. A compromise between the two extremes of no blade avoidance (relatively high collision probabilities near the hub) and complete blade avoidance (zero collision probability near the hub) was implemented in the main model here. That is, if blade avoidance was enabled, the size of the zone was determined by murrelets’ maximum flight speed. However, the resultant collision probability within the zone was not zero, but rather was determined as the product of the unadjusted collision probability and the probability of not avoiding a stationary structure. If blade avoidance was disabled, then collision probability was unaffected by the murrelets’ maximum flight speed and was determined solely by the Tucker model.

Several related examples may help explain the implementation of blade avoidance and its effect on collision probability. Consider conditions of murrelet flight and wind such that at a particular point near the periphery of the rotor, the collision probability is 0.05, and at another point near the hub, the probability is 0.3. “Near the periphery” and “near the hub” are relative terms that, again, depend on the bird’s maximum speed and the rotor speed. Furthermore, consider that the avoidance probability for stationary structures is 0.9. Irrespective of blade avoidance, the collision probability at the point near the periphery remains 0.05; a murrelet cannot fly fast enough to avoid the blades, which have very high tangential velocity. If 100 murrelets were to fly through the rotor at this point under identical conditions, we would expect 95 of them to pass through by chance. At the point near the hub, collision probability depends on murrelet behavior. In the absence of blade avoidance, the bird flies through the rotor on a straight path without altering its speed. In that case, collision probability is 0.3. In other words, 70 of every 100 murrelets would pass through by chance. On the other hand, if blade avoidance is enabled in the model, we assume that the bird can see the approaching blade and take evasive action. Its probability of *not* successfully avoiding an approaching blade is $1 - 0.9 = 0.1$. Thus the resultant collision probability is $0.1 \times 0.3 = 0.03$. That is, of the 30 murrelets that otherwise would have been struck, most (90%, to be precise) are predicted to avoid the oncoming blade.

For the murrelet, enabling blade avoidance generates a large region of low collision probability. This region is larger than for most bird species because murrelets are capable of very rapid flight (maximum speed = 51 m/s in this model).

General Comments on Flight Behavior and Murrelet / Wind Turbine Interactions

All flight paths were modeled independently; in other words, flock behavior was not considered in the model, though similar paths at similar altitudes would be expected to “behave” similarly on average. Flight paths followed straight lines. Once a path entered the wind park, altitude could change (as part of avoidance), but direction did not change nor were there any permanent lateral shifts in the path. Avoidance of a structure encountered along a path was independent of avoidance of any structures subsequently encountered.

Bird encounters with wind turbines followed several straightforward rules. Unsuccessful avoidance of a tower or nacelle was equivalent to a collision. Unsuccessful avoidance of a rotor-

swept disc invoked either the Tucker model or the lookup table based on the stationary rotor model to determine probability of collision with a blade or the hub. A collision terminated the flight path, i.e., it was considered equivalent to death.

There were no edge effects of any kind. Birds were treated as points moving along 1-dimensional paths. A path either intersected a structure (including rotor-swept discs) or not and, if so, a collision either occurred or not. Turbulence effects (in particular, downwind of rotors) were not considered. Winkelman (1994) found that of 10 bird fatalities associated with wind turbine rotors, at least 3 (and possibly as many as 5) were due to the downstream turbulence. We are not aware of other published evidence on this subject. Murrelets are strong, fast fliers, so it is likely that they are less affected by turbulence. Ignoring downstream effects may introduce a negative bias into our estimates of “collision” probability, though we believe any such bias is negligible.

SIMULATION PROTOCOL

For each simulation, the initial number of murrelets was adjusted to ensure that an adequate number of murrelet flights passed through the wind park at heights within the zone of risk (i.e., below the maximum rotor height). More specifically, the initial number was chosen such that on average, at least 100 birds would have been at direct risk of colliding with a wind turbine.

In all simulations avoidance probability for active rotors was held at 0.75 and stationary structure avoidance (for towers, nacelles, and stationary rotors) was fixed at 0.9. Other simulation parameters that were directly controlled included: (1) wind turbine configuration – an array of either 27 large or medium (3 MW) wind turbines, or 32 small (1.5 MW) wind turbines; (2) blade avoidance (either enabled or disabled); (3) curtailment strategy (either no curtailment, 80/80 curtailment in the morning only, or 80/80 morning and evening); and, (4) season (either winter or breeding season). In addition, during July only (a portion of the breeding season), we simulated 2 periods of the day (either morning or evening); for winter only one period (morning) was considered. Thus, there were $54 = (3 \times 2 \times 3 \times 3)$ combinations of all parameter values, i.e., 54 separate simulation runs.

A simulation consisted of 1000 iterations. That is, collision probabilities were estimated 1000 times for each of the 54 combinations of parameter values. At the onset of each iteration, several steps were followed based on the selected simulation parameters: (1) wind speed and direction were randomly selected from the met tower data based on the chosen season and period of the day; (2) wind turbines were rotated to face into the wind, and wind turbine rotational velocity was calculated from the selected wind speed; (3) flight heights were generated for all murrelets from the appropriate lognormal distribution; (4) murrelets with heights exceeding maximum rotor height were “removed”, leaving N_r birds at risk; (5) air speeds were independently selected for all birds at risk by generating random variates from the modified Gamma distribution; (6) flight directions were independently selected for all birds at risk by randomly sampling from the appropriate distribution for the chosen season; (7) for each direction of approach to the wind park, bird flight path origins were randomly generated from a Uniform distribution across the “width” of the park (e.g., Figure 14).

For each of the N_r murrelets at risk, its path was examined to determine the intersections (or encounters) with structures in the wind park. Each encounter along the path was successively evaluated by generating a uniform random variate to compare to the relevant avoidance probability or, for encounters with rotor components (based on either the Tucker model or the lookup table for stationary rotors), to the resultant collision probability. Whenever a collision occurred or the path through the wind park was completed without any collision events, the next flight path was similarly evaluated. When all N_r flight paths had been evaluated at the end of an iteration, the total number of collisions was tallied. The total probability of collision was calculated as $p_c = n_c/N$, the proportion of birds that collided with a structure among all birds, including those that flew above maximum rotor height.

ANALYSIS METHODS

Summary of Collision Probability Estimates

Results were summarized across all iterations for each simulation (each combination of avoidance probabilities, curtailment strategy, season, and period of the day). Mean values of collision probabilities were calculated. In addition to overall probabilities, the mean probabilities of collision with individual structures (rotor, tower, and nacelle) were calculated.

Passage Rate Estimation

Expected numbers of murrelet flight paths in the wind park were estimated using detection rates of murrelet-type targets from the radar studies conducted in 2007 – 2009 (Hamer Environmental 2009). Passage rate estimates were based on targets that met the filtering criteria for flight direction (see *Murrelet Characteristics / Flight Direction* above) and crossed the ridge-top during the period from 105 minutes before sunrise until 30 minutes after sunrise. Pre-sunrise detections were considered more likely to be murrelets than those detected later in the morning, though the period was extended for ½ hour to account for outbound murrelets. At more typical east-west oriented valley locations where murrelets are breeding, most pre-sunrise flights are inbound (east bound ± 45 degrees), while outbound flights (west bound ± 45 degrees) predominate after sunrise (Cooper et al. 2001). Passage rates in these locations are often calculated by using pre-sunrise inbound rates and multiplying by 2 to estimate the number of murrelets returning to sea by the same path while helping to avoid target confusion with the larger number of diurnally active birds flying post sunrise. However, at RRWRA it was not possible to define inbound and outbound flight directions using typical east and west criteria due to the orientation of the ridge-top and the surrounding water bodies. The ridge-top, which runs northwest-southeast, is surrounded on two sides by water (Willapa Bay and the Columbia River Mouth). Therefore, murrelets could be approaching the ridge-top from a variety of angles for both inbound and outbound flights. As a result, at RRWRA the definition of murrelet-type targets could not be restricted to inbound flight paths. Therefore, we expect that a small proportion of the murrelet-type targets flying over the ridge-top pre-sunrise were not murrelets. We also expect that proportion increases post-sunrise. Including all pre and post sunrise targets from all flight directions would certainly over estimate murrelet passage at RRWRA. Thus, we believe that extending the period for daily passage rate estimation by ½ hour post-sunrise represents a conservative choice (still likely to over-estimate the murrelet passage rate). That is,

it would include additional murrelet flights through the wind park, but would also likely include other non-murrelet targets.

We assumed that all flights through the wind park would occur in the morning, except in July (peak breeding season) when 70% of flights would occur in the morning. That is, radar surveys conducted in July in the morning would miss the 30% of flights that occurred at other times of the day, primarily in the evening. Therefore, the July evening passage rate was calculated from the observed morning passage rate as:

$$\text{Evening Passage Rate} = (\text{Morning Passage Rate}) \times 3/7$$

The assumption that in July all murrelets pass through the park in the late afternoon/early evening, if not the early morning, is certainly an over-simplification of murrelet flight patterns, but is likely to over-estimate numbers of fatalities. As explained above, wind speeds were generally higher in the late afternoon than at other times of day. Furthermore, unless murrelets are flying directly downwind, higher wind speed generally leads to higher probability of collision with wind turbine rotors, within the range of wind speeds typically observed during the breeding season. Therefore, collision probabilities and relative numbers of fatalities are expected to be somewhat higher in the late afternoon/early evening than at other times of day.

Flock Size

Passage rates were adjusted to account for the fact that murrelets flying close together may appear as one target on radar. Based on a study combining radar and visual observations of murrelets, mean “flock size” has been estimated as 1.46 murrelets per radar target (Brian Cooper, ABR Inc., unpublished data). Therefore, passage rates estimated as described above were multiplied by 1.46.

Radar Coverage

Marine radar surveys were conducted with the radar range set at 1.5 km, so that the “front” available for passage of murrelet-type targets was 3 km. This distance was less than ½ the straight-line distance (6.685 km) of the proposed wind turbine string along the ridge-top. Therefore, to estimate passage rates through the wind park, radar passage rates were multiplied by 2.23 (=6.685/3). Passage rates by season and period of the day are summarized in Table 3; these estimates include adjustments for flock size and radar coverage.

No Adjustment in Passage Rate Due to Wind Park Fatalities

Realistic estimates of murrelet passage rates would include adjustment for fatalities due to collision with wind turbines. That is, such losses ought to lead to lower passage rates, assuming collision was the only factor causing a change in the population size. However, estimating the size of the effect would require knowledge of local population size, population trend, and the number of times each day that an individual murrelet in the population passed through the RRWRA. Because none of these quantities was known, we made no corresponding adjustment.

Thus, our passage rate estimates applied to an operational wind park are likely biased high. Similarly, the predicted number of fatalities per year (see below) will likely be over-estimated.

Fatality Estimation

Fatality estimates were calculated as the product of collision probability and passage rate for all simulation conditions (i.e., all combinations of wind turbine configuration, avoidance probabilities, curtailment strategy, season, and period of the day). Annual estimates of fatality were obtained by summing across season and period of the day.

RESULTS

Simulation results have been summarized for each combination of wind turbine design, season, period of the day, blade avoidance (either disabled or enabled), and curtailment strategy (Table 4). Each value shown represents the mean of 1000 simulations. Across all combinations of simulation conditions, mean collision probability ranges from approximately 0.00016 to 0.00056. In other words, for any particular set of conditions, as few as 16 out of every 100,000 murrelets, or as many as 56 out of every 100,000, would be expected to collide with a wind turbine.

In general, collision probabilities are very similar for the small (1.5 MW, 77 m rotor) and medium (3.0 MW, 90 m rotor) wind turbines, Figure 15. Recall that the wind park layout for the small wind turbine includes 32 wind turbines, while the layout for both the medium and large wind turbines includes 27 wind turbines. Thus, in comparing results for the small and medium designs, it appears that the smaller size is offset by the greater number such that collision risk is little affected by these 2 wind turbine size/layout alternatives. On the other hand, collision probabilities are greater for the large (3.0 MW, 101 m rotor) wind turbines (Figure 15). Typically, these probabilities are 25% greater than for either the small or medium wind turbines. In comparing medium and large wind turbines, the differences in collision probability are undoubtedly attributable to rotor size (both maximum extended blade-tip height and rotor-swept area) alone since all other design features are identical.

Collision probabilities are greater for winter than for the breeding season (Table 4, Figure 15). This difference is likely due to seasonal differences in wind conditions, in particular, wind speed. Wind speeds are higher in winter than in the breeding season (Figures 3 and 4). Furthermore, higher wind speed leads to higher wind turbine rotational velocities, for wind speeds up to approximately 12 m/s. All else being equal, higher rotation velocity leads to higher collision risk under the Tucker model. Seasonal differences in wind direction may also contribute to differences in collision probabilities. However, this effect is more difficult to assess than for wind speed, in part because it will depend on interaction with any seasonal changes in murrelet flight directions. Within the breeding season, period of the day has little, if any, discernible effect on collision probability (Figure 15). In this case, the diurnal differences in wind speed (Figures 3 and 4) are likely too small to affect risk.

Blade avoidance allows birds to evade slowly moving blades as they fly through the rotor-swept area near the hub. Enabling this form of avoidance may have a substantial effect on collision

probability (Table 4, Figure 15) depending on curtailment strategy (discussed below). In the absence of curtailment, enabling blade avoidance typically decreases collision risk by 15% – 30%.

Curtailment strategy also has a large effect on collision risk (Table 4, Figure 15). Adopting the 80/80 strategy, such that wind turbines are disengaged 64% of the time during the breeding season, reduces collision probability 50% – 60% relative to the no curtailment strategy. This large reduction in risk emphasize the fact that – as modeled here – overall collision risk primarily reflects the risk of collision with active rotors. Stationary rotors, towers, and nacelles each contribute relatively little to overall risk.

Predicted fatalities are calculated as the product of collision probability and passage rate, by season and period of the day. Summing these seasonal and diurnal estimates yields annual fatality estimates (Table 5). Generally, fatalities follow patterns similar to those for collision probabilities, though there are 2 primary exceptions. First, in the absence of curtailment and blade avoidance, there are slightly more predicted fatalities in the breeding season than in winter, even though collision probability is higher in winter (Table 4) and the winter is longer (Table 3). This result occurs because estimated daily passage rates are greater in the breeding season. Second, while collision probabilities are similar for the morning and evening periods (Table 4), there are few fatalities in the evening (Table 5). This result clearly is due to both the low estimated passage rate per evening and the short period (31 days) in which evening flights are assumed to occur. Otherwise, as with collision probabilities, lower fatalities are associated with smaller turbines, more stringent curtailment in the breeding season, and blade avoidance.

Predicted fatalities are less than 1 per year for all simulation conditions that were examined. Consistent with the model results for collision risk (Table 4), predicted numbers of fatalities are very similar for the small and medium wind turbines, at most 0.59 per year under the assumptions of no blade avoidance and no curtailment. For the large wind turbines, annual fatalities are predicted to be as high as 0.72 per year. Curtailment reduces these predictions. For instance, for the large wind turbines 80/80 curtailment in the morning only leads to 0.60 predicted fatalities per year. Interestingly, additional curtailment in the evening has only a very small effect on predicted fatalities. While evening curtailment does affect collision probability, estimated evening passage rates are relatively low and evening flights are assumed to occur only in July, a small proportion of the breeding season. Thus, the net effect on total predicted fatalities is negligible. Presuming murrelets actively avoid oncoming blades as they fly through the rotor-swept area also leads to lower predicted fatalities, under the no curtailment strategy, predicted annual fatalities are 20% - 30% lower with blade avoidance compared to the no avoidance assumption.

References

- Batschelet, E. 1981. *Circular Statistics in Biology*. Academic Press, London.
- Chinook Wind. 2008. Quarterly Validated Data Report: Radar Ridge, Second Quarter. Prepared for Energy Northwest.
- Cooper, B.A., M.G. Raphael, and D.E. Mack. 2001. Radar-based monitoring of marbled murrelets. *Condor* 103:219-229.
- Elliot, D.L., C.G. Holladay, W.R. Barchet, H.P. Foote, W.F. Sandusky. 1986. *Wind Energy Resource Atlas of the United States*. Pacific Northwest Laboratory, Richland, Washington. Prepared for: U.S. Department of Energy.
- Elliot, K.H., M. Hewett, G.W. Kaiser, and R.W. Blake. 2004. Flight energetics of the Marbled Murrelet, *Brachyramphus marmoratus*. *Canadian Journal of Zoology* 82:644-652.
- Hamer Environmental. 2009. Use of Radar to Determine Passage Rate and Height Distributions of Marbled Murrelets at the Proposed Radar Ridge Wind Resource Area, Pacific County, Washington. Draft report prepared for Energy Northwest.
- Hansen, M.O.L. 2008. *Aerodynamics of Wind Turbines*, 2nd edition. Earthscan, Sterling, VA.
- Hansen, M.H., A. Hansen, T.J. Larsen, S. Øye, P. Sørensen, and P. Fuglsang. 2005. Control design for a pitch-regulated, variable speed wind turbine. Risø National Laboratory, Roskilde, Denmark.
- Petersen, I.B., T.K. Christensen, J. Kahlert, M. Desholm, and A.D. Fox. 2006. Final results of bird studies at the offshore wind farms at Nysted and Horns Rev, Denmark. National Environmental Research Institute, Denmark.
- Sibley, D.A. 2003. *The Sibley Field Guide to Birds of Western North America*. Alfred A. Knopf, New York.
- Tucker, V.A. 1996. A mathematical model of bird collisions with wind turbine rotors. *Journal of Solar Energy Engineering* 118:253-262.
- Winkelman, J.E. 1994. Bird/wind turbine investigations in Europe. Pages 43-48 in Proceedings of the National Avian-Wind Power Planning Meeting, Denver, CO, 20-21 July 1994.

Table 1. Wind turbine characteristics used in the collision model. Those dimensions not meeting manufacturer specifications were either close to manufacturer specification, inferred from other dimensions, or assumed.

Feature (dimensions)	Vestas V90, 3 MW (Large / Medium)	GE 1.5sle (Small)
Tower diameter (m)		
Base	3.7	4.6
Top	2.3	2.6
Tower height (m)	77.5	77.5
Nacelle (L×W×H, m)	9.65 × 3.60 × 4.05	8.84 × 3.51 × 3.86
Hub height (m)	80	80
Rotor radius (m)	50.5 / 45.0	38.5
Cut-in wind speed (m/s)	3.5	3.5
Cut-out wind speed (m/s)	25	25
Rated wind speed (m/s)	15	15
Minimum rotational speed (rpm)	8.6	10
Rated rotational speed (rpm)	16.1	18.4
<i>Features used in stationary rotor model</i>		
Hub diameter (m)	2.5	2.5
Blades		
Total length (m)	49.5 / 44.0	37.5
Shank length (m)	2.0	2.0
Shank diameter (m)	1.9	1.9
Maximum chord (m)	3.9 / 3.5	3.0
Distance, root to max chord (m)	11.2 / 10.0	8.5
Tip chord (m)	0.44 / 0.40	0.35
Tip depth (m)	0.02	0.02

Table 2. Comparison of observed flight height distribution and simulation distribution. Observed distribution for murrelet-type targets, estimated from marine radar in vertical mode. Simulation from a Lognormal(5.57,0.558) distribution.

Distribution	Mean (m)	SD (m)	Proportion Below Max Rotor Height ¹	
			Large (130.5 m)	Small (118.5 m)
Observed	307.9	181.3	0.105	0.079
Lognormal	306.6	185.3	0.105	0.077

¹ Proportion of the distribution at risk of collision, not considering other factors such as avoidance probabilities.

Table 3. Estimated murrelet-type target passage rates through RRWRA by season and period of the day (as defined for collision simulations). For period of the day, AM represents 04:00 – 07:00 in the breeding season and 05:00 – 08:00 in winter, and PM represents 20:00 – 23:00. Total annual passage rates include adjustments for flock size and radar coverage.

Season	Period of Day	Daily Passage Rate	Number of Days at Risk	Total Annual Passage Rate	
				Unadjusted	Adjusted
Breeding	AM	1.89	117	221.1	720.0
	PM	0.81	31	25.1	81.8
Winter	AM	0.98	186	182.3	593.5

Table 4. Mean collision probabilities from 1000 model simulations.

Turbine Design	Season	Period of the Day	Blade Avoidance	Curtailment	Collision Probability
Small GE 1.5 MW 77 m rotor	Breeding	AM	No	None	0.00037008
				80/80	0.00023362
		Yes	None	0.00028604	
			80/80	0.00018967	
		PM	No	None	0.00035466
				80/80	0.00023130
	Yes	None	0.00029067		
		80/80	0.00021434		
	Winter	AM	No	None	0.00042945
			Yes	None	0.00038011
Medium V90 3.0 MW 90 m rotor	Breeding	AM	No	None	0.00039522
				80/80	0.00021783
		Yes	None	0.00028033	
			80/80	0.00018290	
		PM	No	None	0.00039522
				80/80	0.00022518
	Yes	None	0.00030790		
		80/80	0.00019853		
	Winter	AM	No	None	0.00046415
			Yes	None	0.00038695
Large V90 3.0 MW 101 m rotor	Breeding	AM	No	None	0.00048842
				80/80	0.00032632
		Yes	None	0.00034632	
			80/80	0.00023684	
		PM	No	None	0.00043579
				80/80	0.00031579
	Yes	None	0.00038000		
		80/80	0.00023474		
	Winter	AM	No	None	0.00056000
			Yes	None	0.00045684

Table 5. Predicted fatalities based on modeled collision probabilities (Table 4) and estimated passage rates (Table 3).

Turbine Design	Season / Period of Day	No Blade Avoidance			Blade Avoidance		
		No Curtailment	80/80 Curtailment		No Curtailment	80/80 Curtailment	
			AM Only	AM & PM		AM Only	AM & PM
Small	Breeding/AM	0.266	0.168	0.168	0.206	0.137	0.137
	Breeding/PM	0.029	0.029	0.019	0.024	0.024	0.018
	Winter/AM	0.255	0.255	0.255	0.226	0.226	0.226
	Total Annual	0.550	0.452	0.442	0.455	0.386	0.380
Medium	Breeding/AM	0.285	0.157	0.157	0.202	0.132	0.132
	Breeding/PM	0.032	0.032	0.018	0.025	0.025	0.016
	Winter/AM	0.275	0.275	0.275	0.230	0.230	0.230
	Total Annual	0.592	0.465	0.451	0.457	0.386	0.378
Large	Breeding/AM	0.352	0.235	0.235	0.249	0.171	0.171
	Breeding/PM	0.036	0.036	0.026	0.031	0.031	0.019
	Winter/AM	0.332	0.332	0.332	0.271	0.271	0.271
	Total Annual	0.720	0.603	0.593	0.552	0.473	0.461

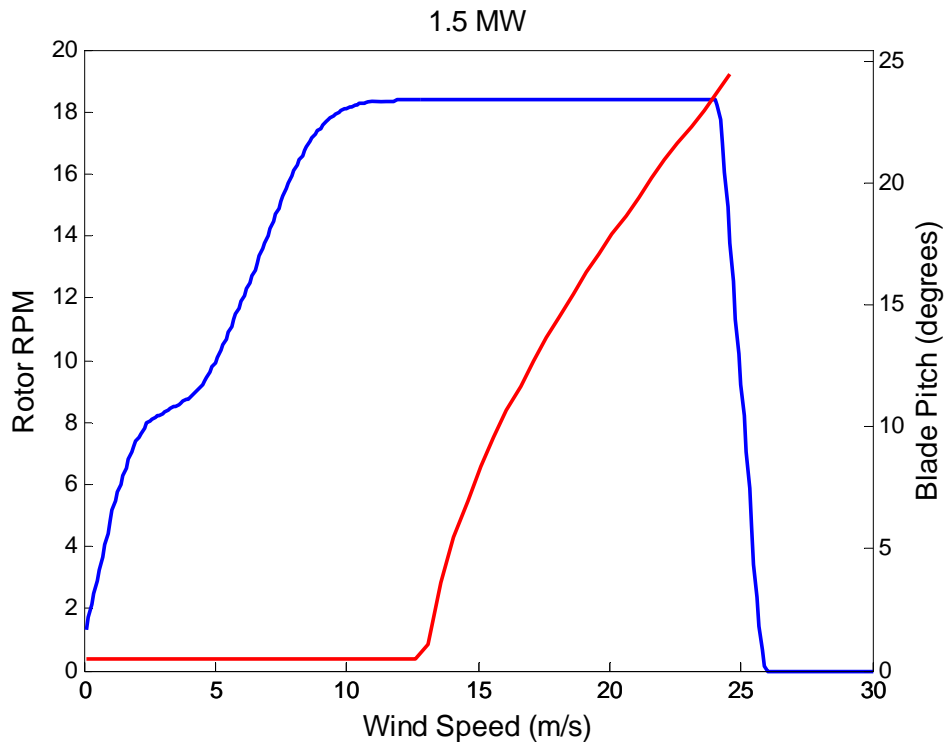
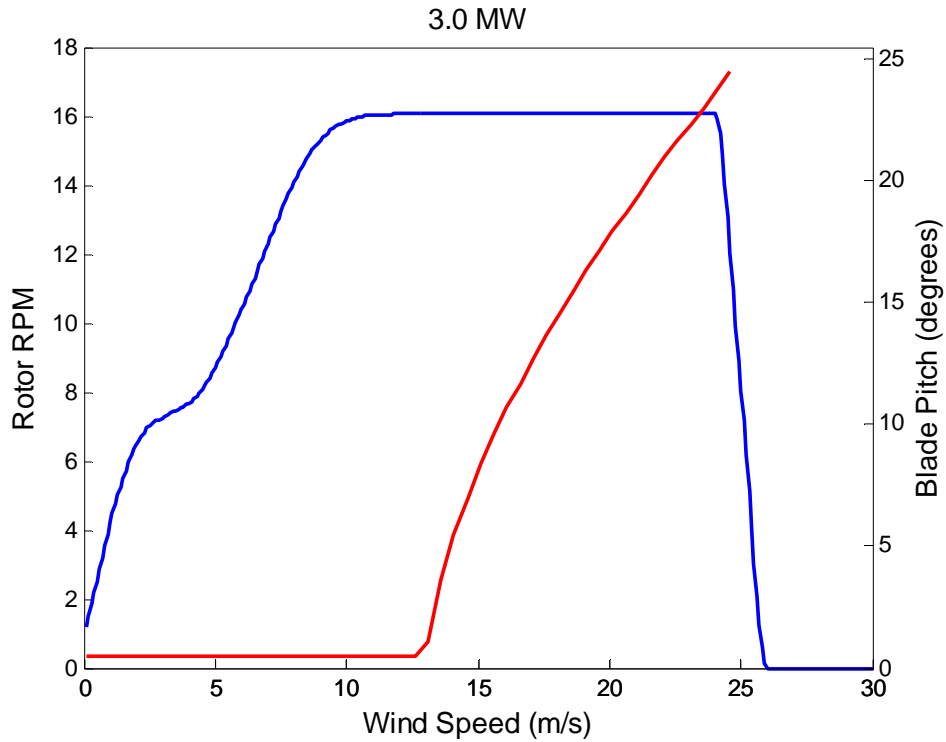


Figure 1. Relationship between wind speed and both rotor speed (blue lines) and blade pitch (red lines) for wind turbine designs used in the collision model (3.0 MW represents both medium and large wind turbines). Note that pitch was assumed to be 90° when the rotors were not turning, though this is not shown.

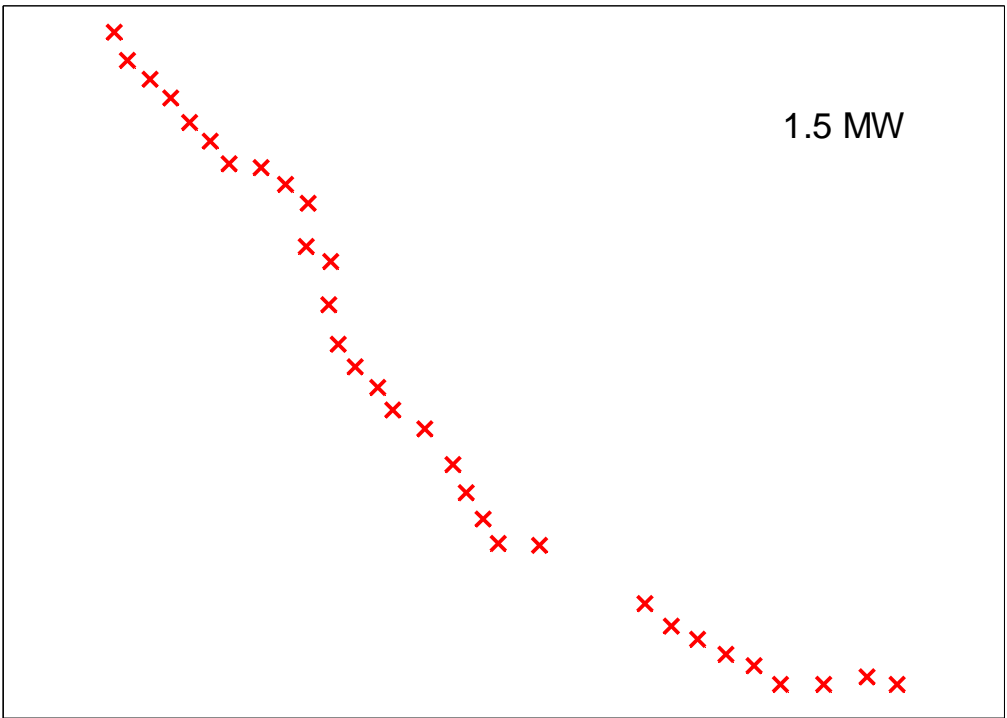
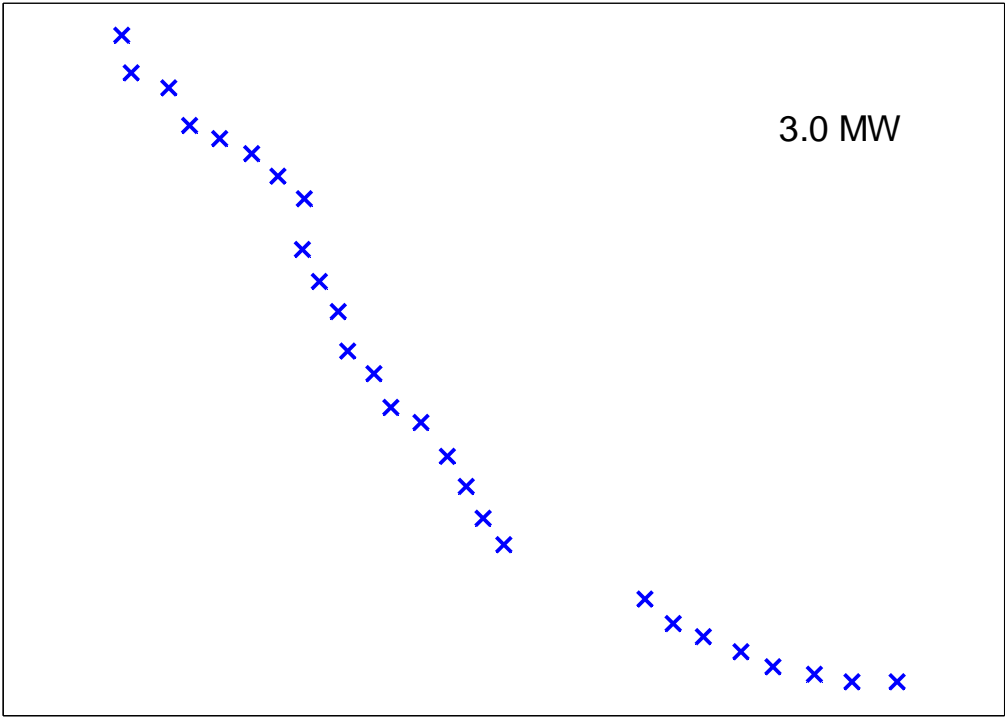


Figure 2. Alternative wind turbine layouts depending on wind turbine design: 3.0 MW layout for large and medium wind turbines; 1.5 MW layout for small wind turbines.

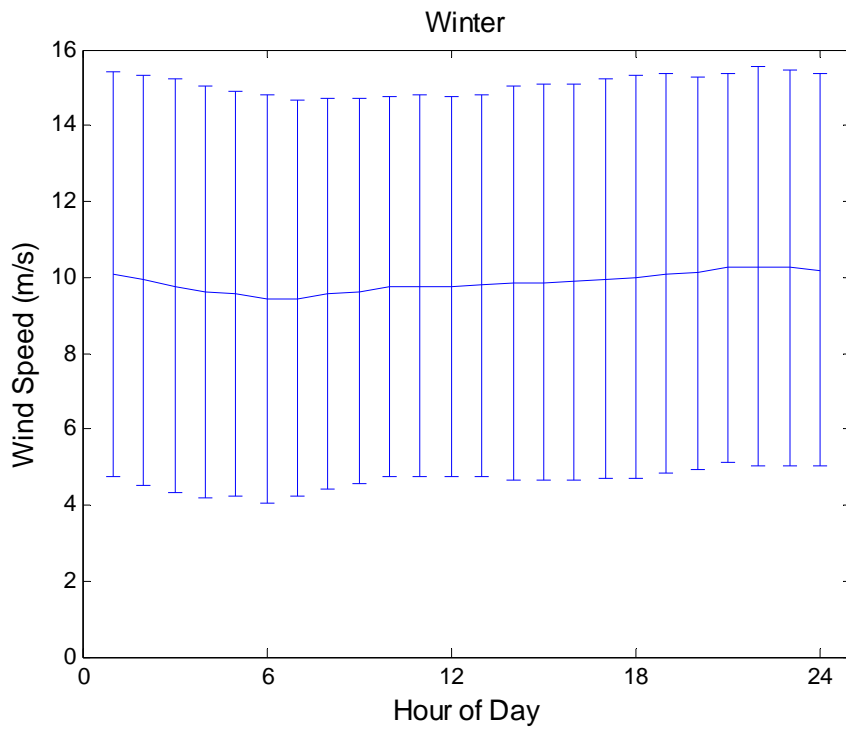
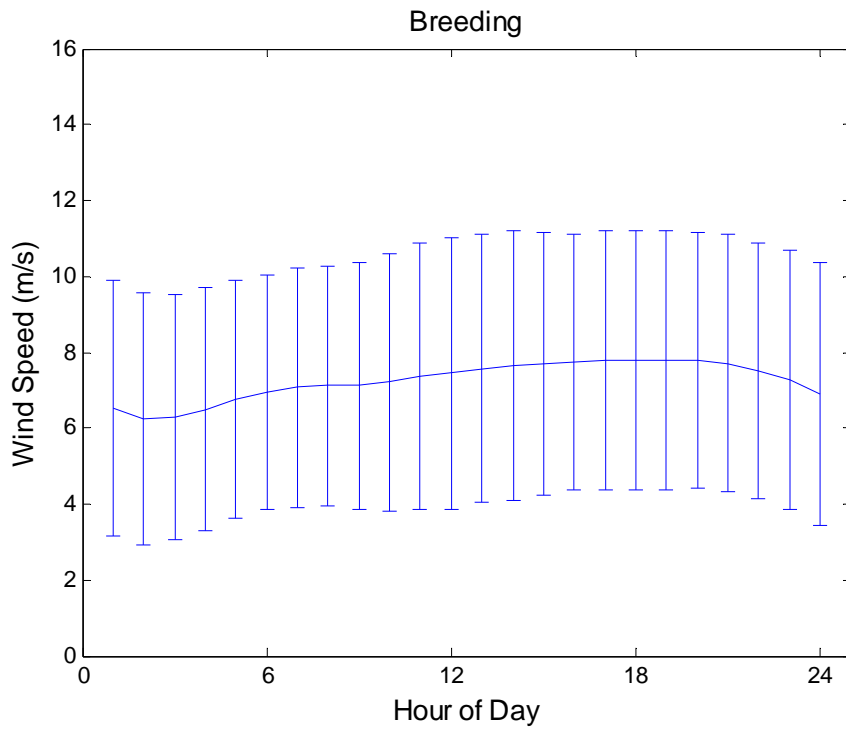


Figure 3. Mean and standard deviation of wind speed by season and hour of the day at Met Tower 801.

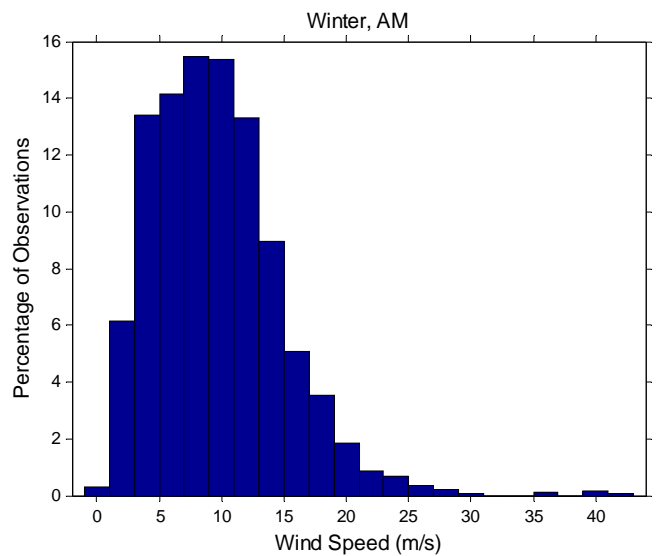
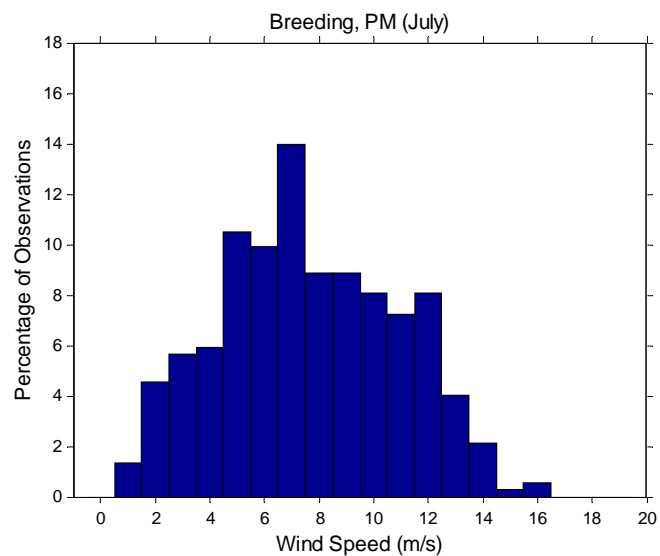
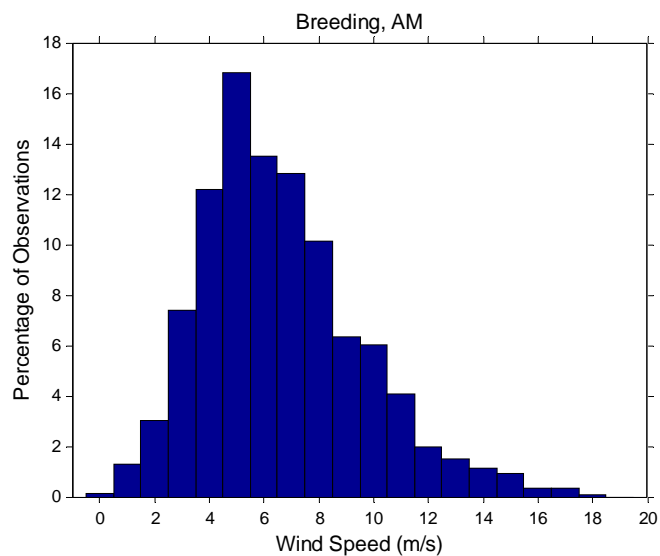


Figure 4. Histograms) of wind speed by season and period of the day. Note different X-axis scales for breeding season and winter.

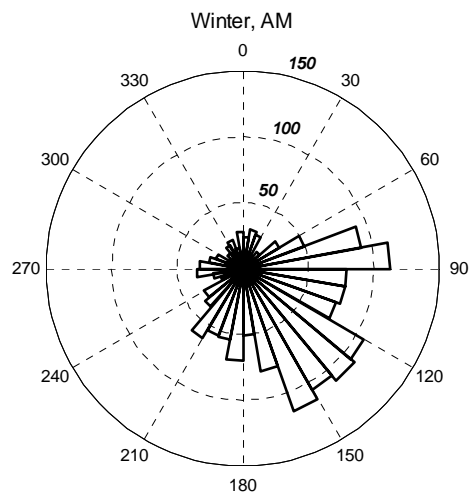
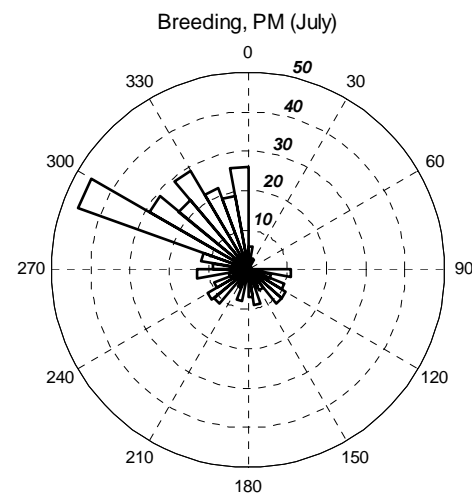
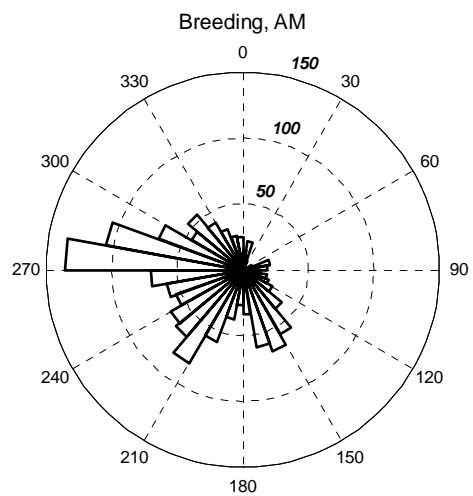


Figure 5. Rose plots (circular histograms) of wind direction by season and period of the day. Wind blows *from* the indicated direction.

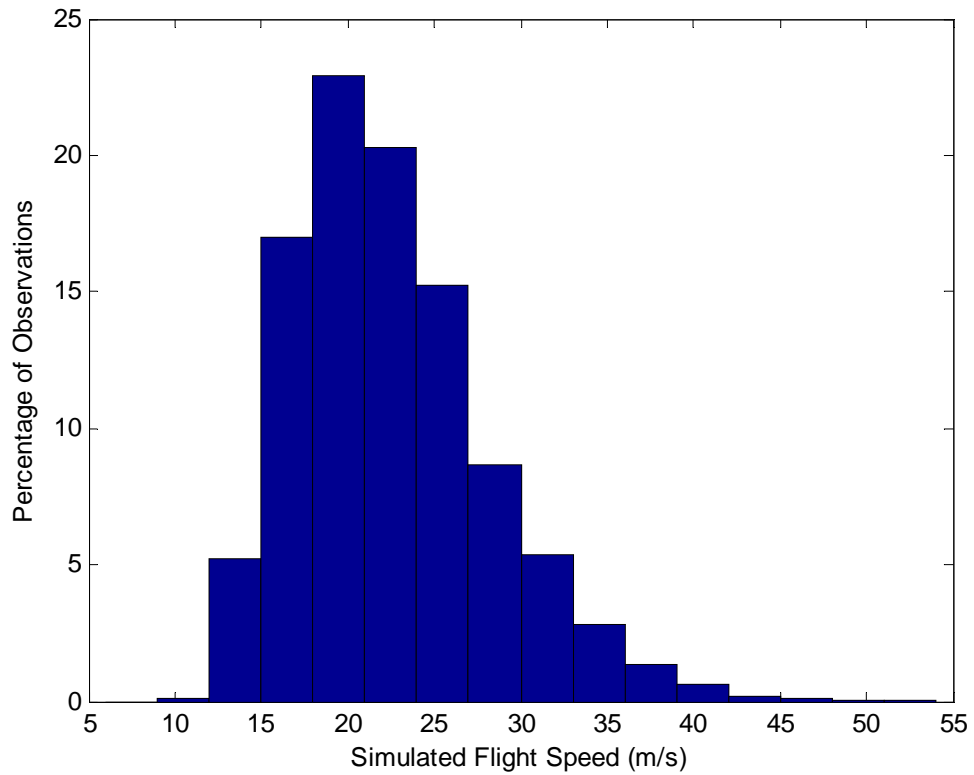


Figure 6. Distribution of simulated flight speed, based on radar observations of murrelet-type targets flights (Elliot et al. 2004). In simulations, maximum speed was truncated at 51 m/s.

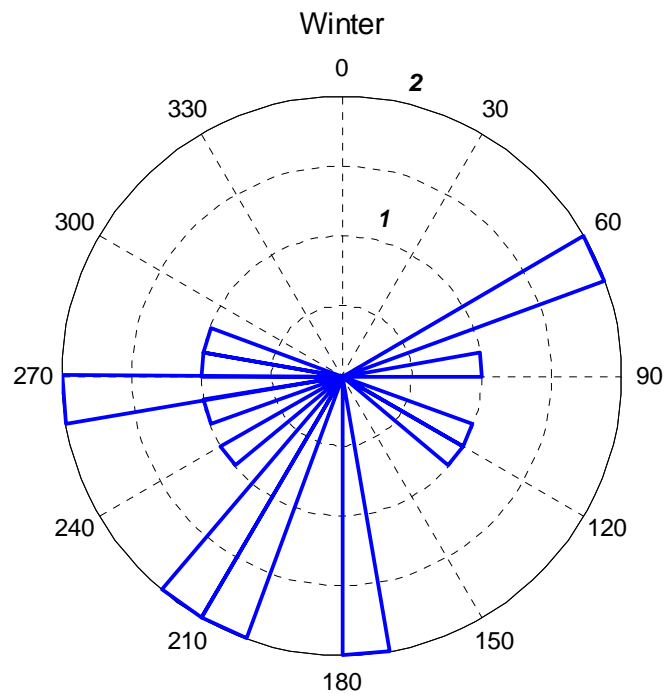
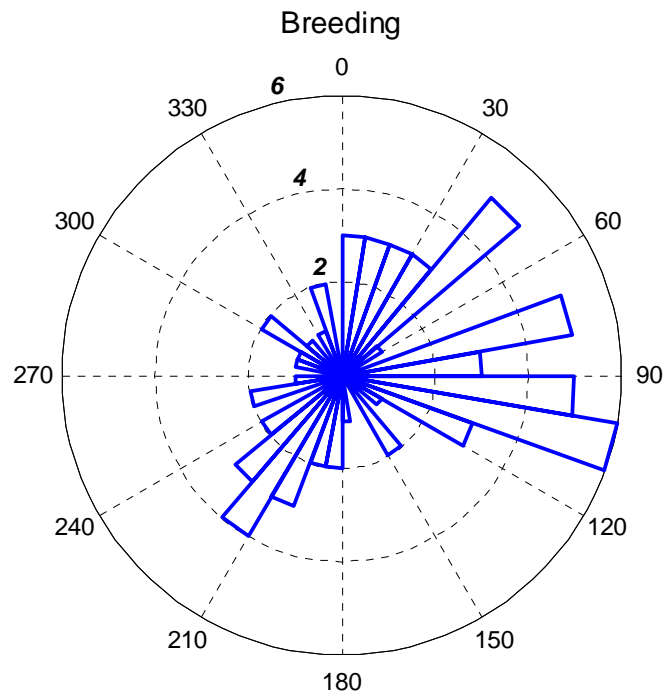


Figure 7. Flight directions of murrelet-type targets observed via marine radar. Murrelets fly *from* the indicated direction (data originally recorded as headings).

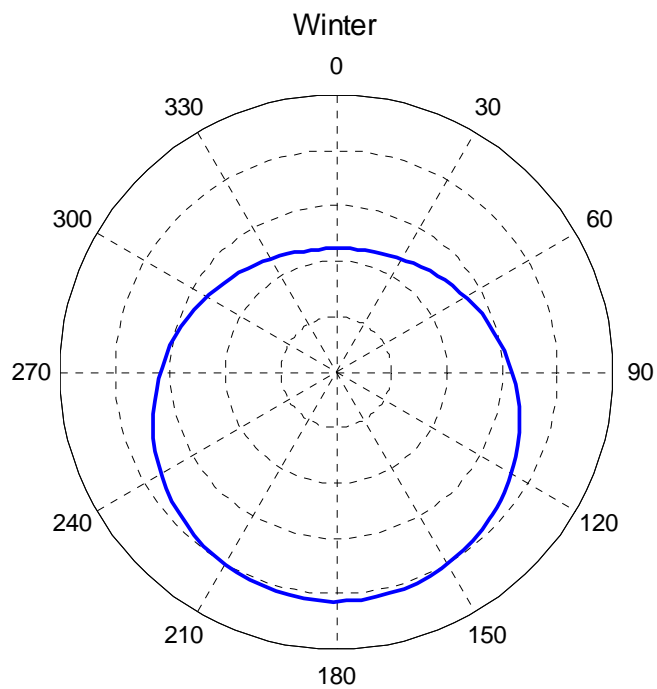
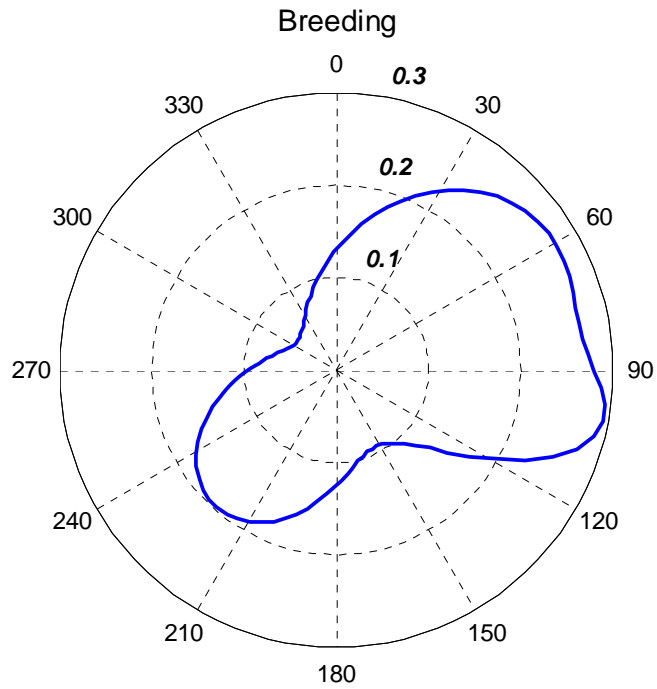


Figure 8. Distributions for simulating flight directions: mixture of von Mises distributions for breeding season; cardioid distribution for winter. Based on observed distributions (Figure 7).

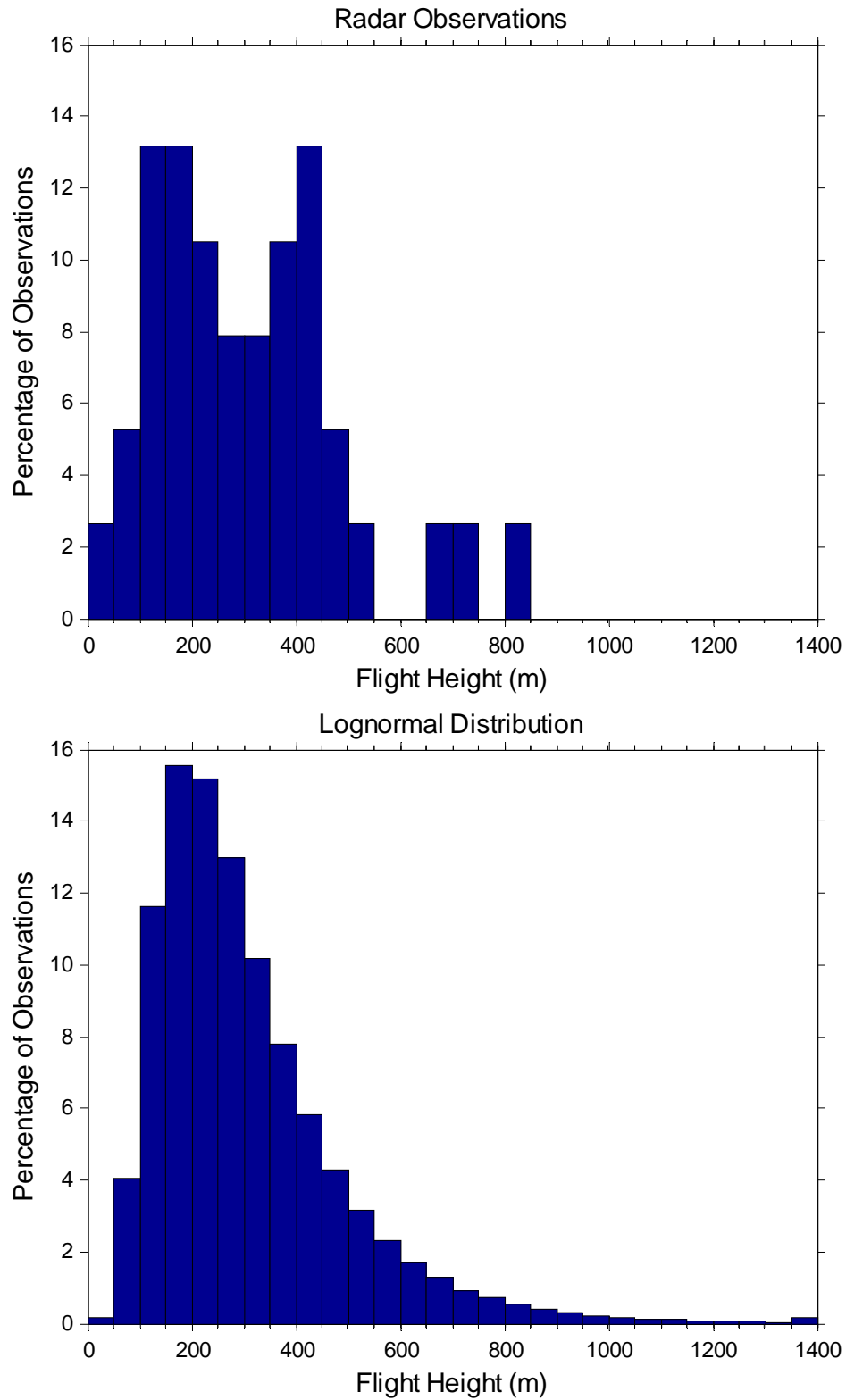


Figure 9. Histograms of observed flight altitudes at RRWRA and the lognormal(5.57,0.558) distribution used for model simulations.

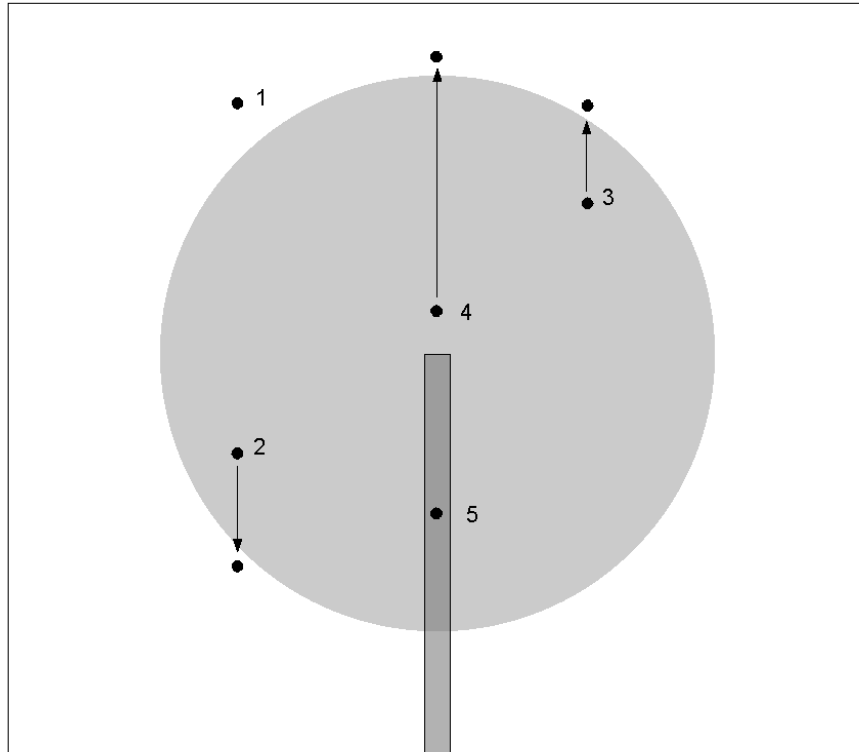


Figure 10. Murrelet / wind turbine interactions, assuming murrelet paths perpendicular to the plane of the rotor. Path 1: murrelet is not at risk of collision with this wind turbine. Paths 2 & 3: rotor avoidance implemented by respective decrease and increase in altitude, with resultant altitude remaining within rotor-swept area heights if other wind turbines are encountered subsequently. Path 4: rotor avoidance implemented by increase in altitude, with resultant altitude above rotor-swept area heights. Path 5: at risk of collision with both rotor and tower.

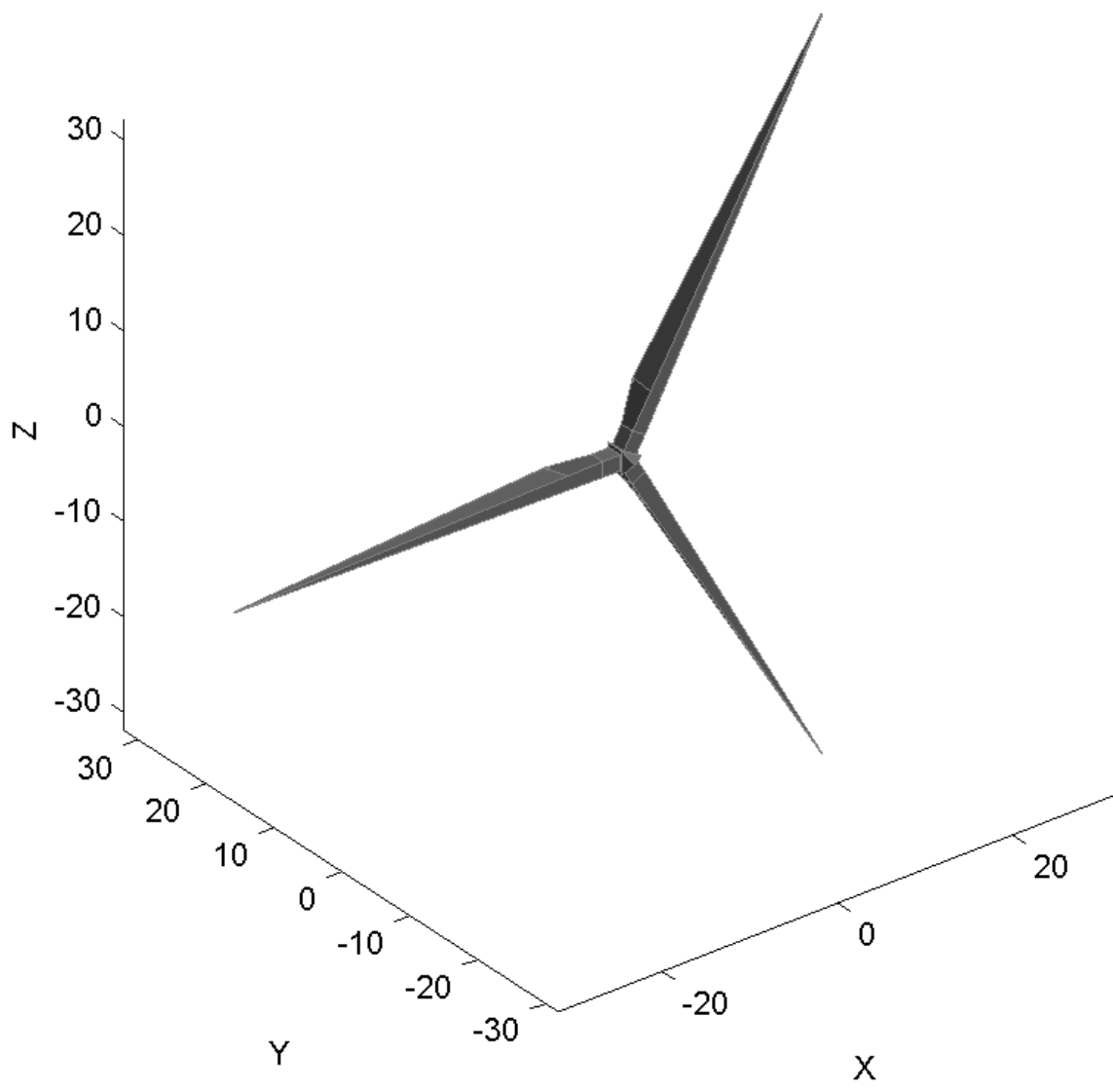


Figure 11. Three-dimensional model used for estimating probability of collision with a stationary rotor.

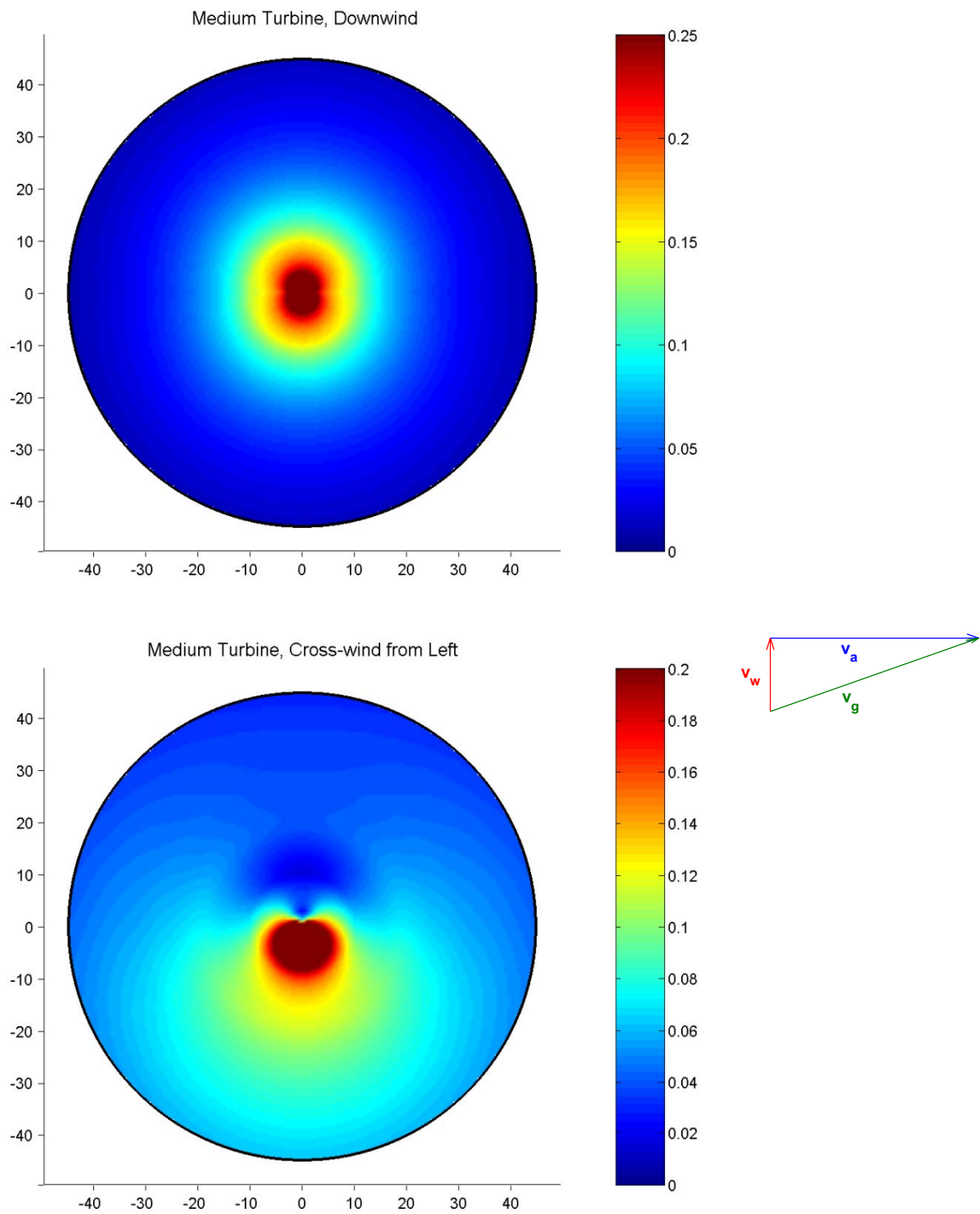


Figure 12. Contours showing probability of rotor blade collision based on Tucker 3-d model, for a 3 MW wind turbine with a 90 m rotor, clockwise rotation. Murrelet: 22.6 m/s airspeed. Wind speed: 8 m/s. Upper panel: downwind flight. Lower panel: crosswind flight. Crosswind vectors: red = wind velocity; blue = bird air velocity; green = bird ground velocity.

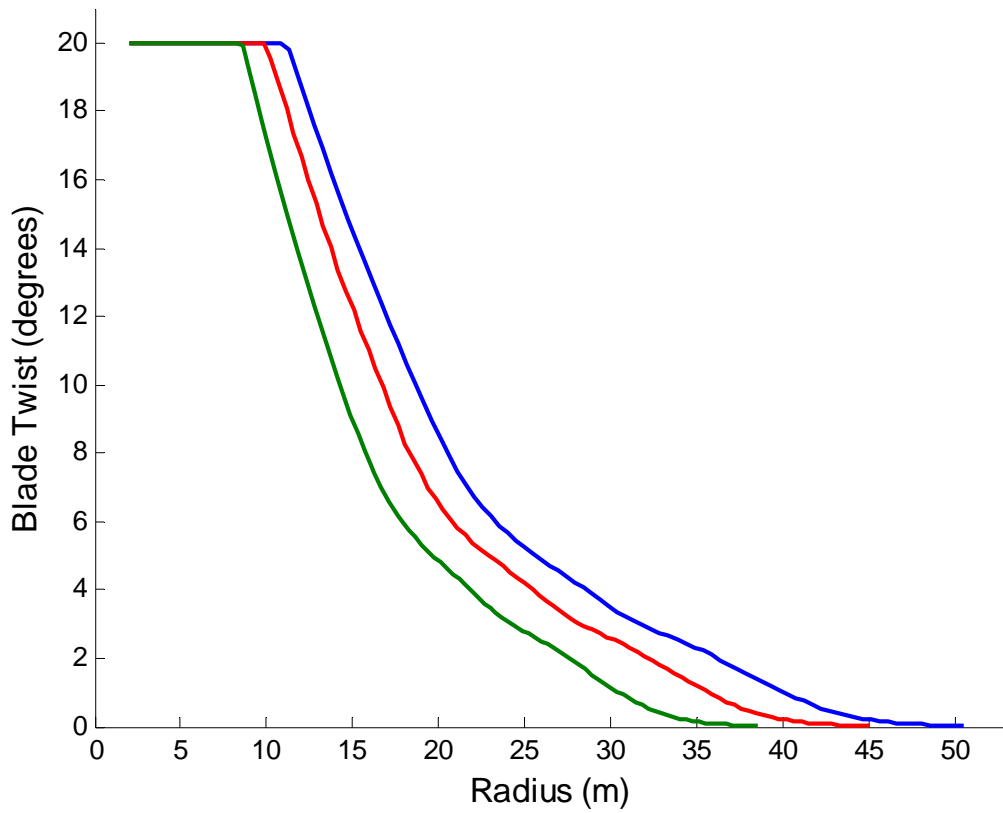


Figure 13. Blade twist as a function of radius for 3 wind turbine designs: green = small (1.5 MW), red = medium (3.0 MW, 90 m rotor), blue = large (3.0 MW, 105 m rotor).

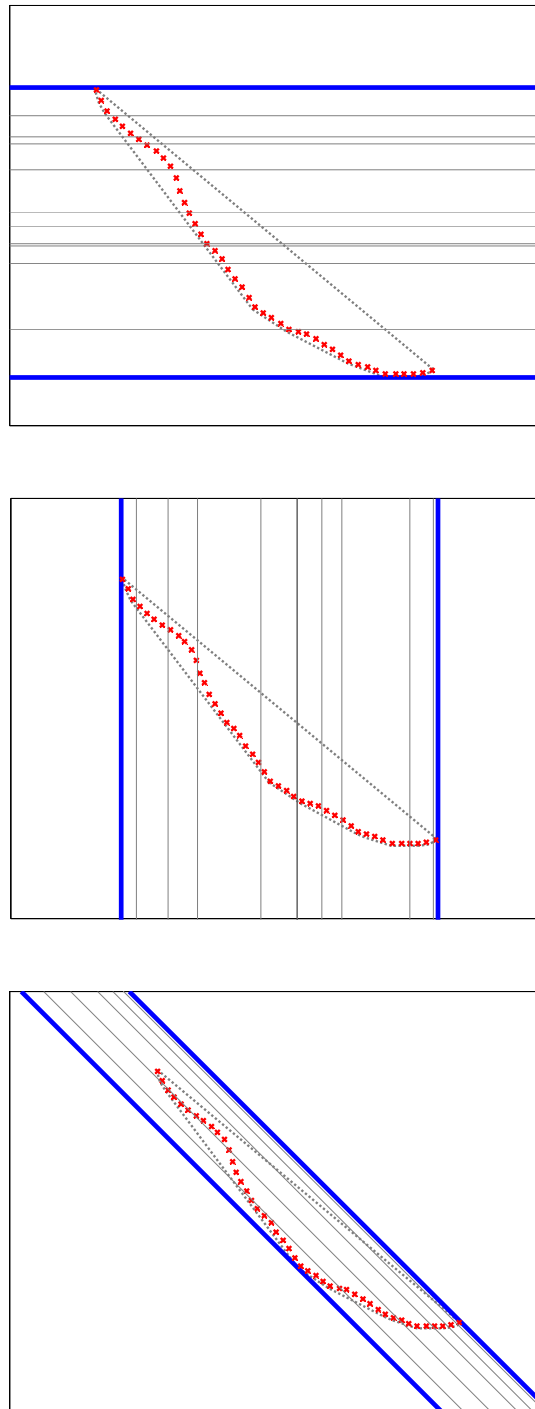


Figure 14. Examples showing simulated murrelet flight paths (thin gray lines) within the width (delimited by thick blue lines) of the wind park assuming flight direction East-West (top panel), North-South (middle panel), and Northwest-Southeast (bottom panel). Red crosses represent wind turbines. Initial positions of flight paths were uniformly distributed within the width of the wind park defined by each selected flight direction.

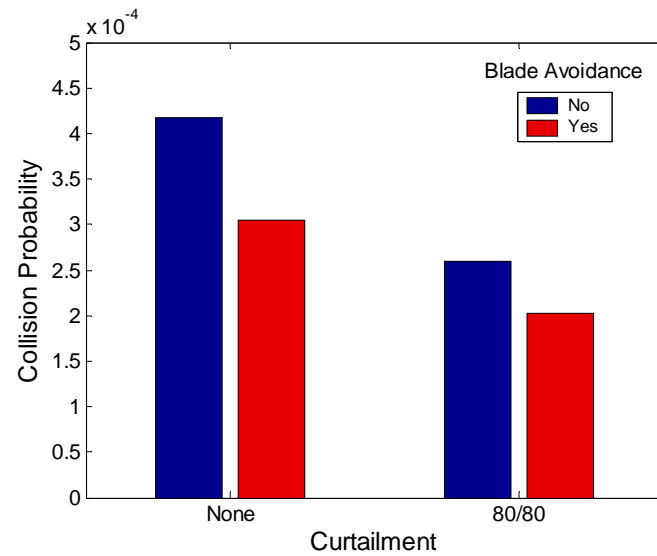
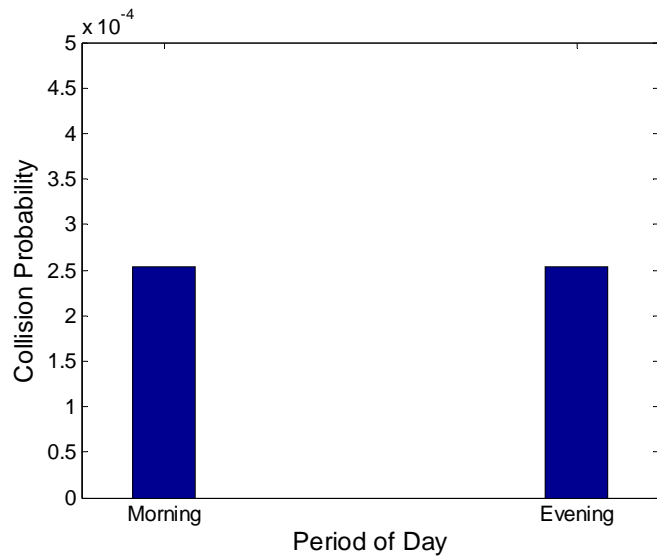
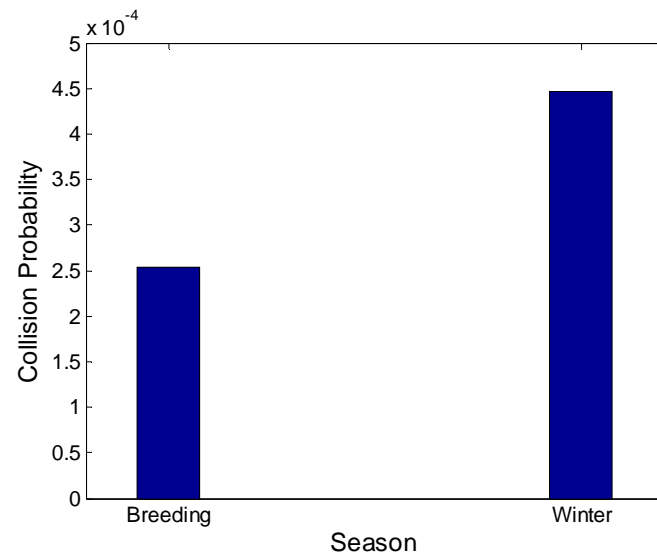
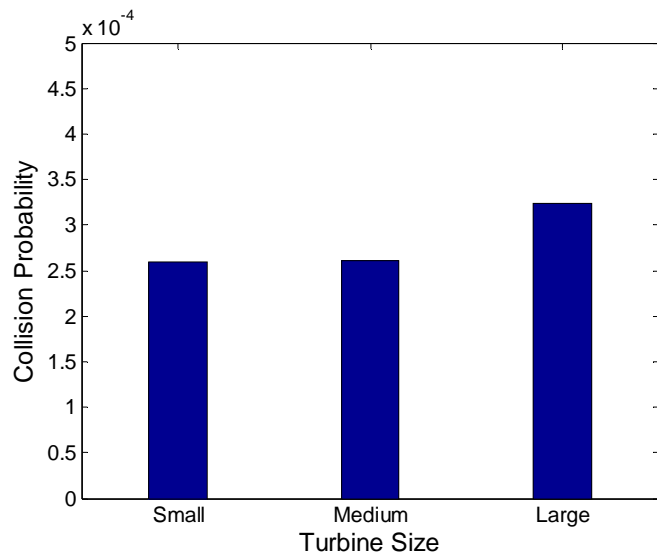


Figure 15. Collision probability as a function of turbine size, season, period of the day (within breeding season only), and both blade avoidance and curtailment strategy (in the morning period of the breeding season only). For each of the plots, collision probabilities in Table 4 were averaged across the remaining factors, e.g., for turbine size, bar heights represent averages across season, period of the day, blade avoidance, and curtailment strategy.